**PAPER** • **OPEN ACCESS**

# Analysis of the impact of precipitation and temperature on the streamflow of the Ürümqi River, Tianshan Mountain, China

To cite this article: Y C Liu *et al* 2018 *IOP Conf. Ser.: Earth Environ. Sci.* **191** 012135



# Analysis of the impact of precipitation and temperature on the streamflow of the Ürümqi River, Tianshan Mountain, China

**Y C Liu[1,4], K Zhao[1], Y Liu[1], X L Yin[2] and D Labat[3,4]**

[1]School of Resources and Environmental Engineering, Jiangxi University of Science and Technology, Jiangxi Ganzhou 341000, Jiangxi Province, China
[2]Guangdong Open Laboratory of Geospatial Information Technology and Application, Guangzhou Institute of Geography, Guangzhou 510070, Guangdong Province, China
[3]Géosciences Environnement Toulouse (GET), Université de Toulouse (CNRS, IRD, OMP), 14 Avenue Edouard Belin, 31400 Toulouse, France

E-mail: liuyoucun@gmail.com/david.labat@get.omp.eu

**Abstract.** This study explores the relationship between streamflow time variability and precipitation and air temperature variability, in the upper reaches of the Ürümqi River in northwestern China. Wavelet analyses are adopted to analyse the multi-time scale features of monthly temperatures, monthly precipitations and monthly runoffs during the years between 1958 and 2006. Results of continuous wavelet transform imply a statistically significant cycle over an approximately 12-month period in the temporal fluctuations of monthly air temperature, precipitation and runoff. Furthermore, monthly temperature shows 66-month and 96-month cycles while monthly precipitation shows 6-month, 30-month and 72-month cycles. Monthly runoff has 6-month, 24-month, 36-month and 72-month cycles. The results of cross wavelet transform and wavelet coherence show that monthly runoff variability correlates with precipitation and air temperature fluctuations at 6-month and 12-month respectively. Other time-scale correlations at 1-year, 2-year, 3-year and 6-year marks are also highlighted between the different time series. These correlations are then explained considering the alpine characteristics of the catchment. Higher air temperatures in the upper reaches of the Ürümqi River accelerate snow melt and intensify evaporation, thus the relationship between air temperature and runoff is uncertain during different seasons. Overall, summer air temperature controls the annual runoff and precipitation provides a sustained water supply to the upper Ürümqi River. They constitute the dominant factors that explain the temporal variations of streamflow in the upper Ürümqi River. Univariate and cross-wavelet analyses on runoff and climate variability clearly offer a useful tool in hydro-meteorological issues in alpine areas.

## 1. Introduction

Runoff is strongly affected by climate change and underlying surface situation [1-4]. The climate change directly influences the volume, temporal and spatial distribution of runoff [5]. The climate factors, such as precipitation, air temperature and evaporation, have a significant influence on the generation of runoff [6-11]. It is noted in the Synthesis Report of IPCC [12] that global climate warming has led to temporal and spatial redistribution of regional water resources in the last century. This is particularly true for glacial streams as the surface runoff volume decreases with the change in generation situation caused by climate warming [9,13]. More specifically, changes in air temperature strongly modulate snow accumulation and melt, thus affecting the hydrological systems which

originate in the alpine regions [14-17]. A number of studies relate meteorological factors to the streamflow in alpine catchments [4,7,15,16,18,19].

Many studies have been conducted to capture the interactions between runoff, air temperature and precipitation in alpine catchments [9,14-16,17, 20-22]. Yet the correlation between the meteorological factors and runoff of the Ürümqi River has rarely been discussed. This is an issue which will affect the evaluation of regional water resources and regional sustainable development in Ürümqi city. The Ürümqi River is located in the arid and semi-arid areas in northwestern China. The runoff is very sensitive to climate changes in the upstream of Ürümqi River, *i.e.*, minor climate change, tend to result in significant fluctuations in the runoff. Due to global warming, the warm and dry climate in the inland mountain areas in northwestern China has gradually transformed into a warm and humid climate [21,23]. The changing precipitation as well as air temperature would affect the runoff of the Ürümqi River. Furthermore, the Ürümqi River which is located in Tianshan Mountain is a large source of water for Ürümqi City [23]. The city houses 3.5 million people [24] and any changes in runoff would have an enormous impact on the daily lives of the local residents. The hydrology process in this catchment as well as its response to climate change has attracted more attention in recent decades, especially the correlation between climate variability and runoff in the upper Ürümqi River.

The interaction between the precipitation or air temperature and runoff in alpine areas is complex. Firstly, the process is highly dependent on topographical features and latitude [15]. Warmer air temperatures at higher elevations may have no impact on snowpack, whereas they would result in earlier melt when they are closer to the snow line [19,25]. Secondly, annual runoff is dominated by mean air temperatures in summer in highly glacierized alpine river basins [15,17]. Thirdly, the physical mechanisms of precipitation-runoff and air temperature-runoff in different alpine regions are different [26]. Over the last decades, air temperature and evaporation have increased with glaciers retreating and permafrost receding in the mid to high latitudes in the northern hemisphere [25].

Wavelet analysis is able to quickly and effectively reflect the features of runoff, air temperature and precipitation regimes as well as their interrelationships [21,27-32]. A number of the latest studies have looked into the correlation between air temperature, precipitation and runoff, and conducted case studies in drainage basins by using wavelet analysis. Examples include [33] Tarim's headwater basin, [24] the alpine meadow belt of the Tianshan Mountain, [21] Aksu River, [34] Quebec and Ontario of Canada, [35] Aegean region of Turkey, [36] Guyana Shield, [32] upper reaches of Danube River, [37] source regions of Yangtze River, [38] Yarkand River. All these studies indicated that wavelet transform is an effective method to analyze the spatial and temporal non-linear relationship of runoff to climate factors in time series.

This study contributes to this cause by investigating the quantitative impact of air temperature and precipitation on the streamflow in mountain drainage basins along the Ürümqi River of Tianshan Mountains, China. Simultaneously, we try to understand the low-frequency fluctuations and their interactions, so as to explore the statistical characteristics of runoff, precipitation and temperature changes over time. Do these time series show long-term correlation? How does the data fluctuate in terms of scale and time? What is the relation between the cycle in discharge and those in precipitation and temperature?

## 2. Field site and data

### *2.1. Field site*

The upper basin of the Ürümqi River is located on the northern slope of the Tianshan Mountains and along the southern edge of the Junggar Basin in Xinjiang, northwestern China [23,39,40]. Basin latitude extends from 43°00' N to 43°28' N and longitude extends from 86°45' to 87°18' E (figure 1). The Ürümqi River originates from Glacier No.1, the northern wing of the Tianger Peak II (4479 m ASL) in the middle of the Tianshan Mountains [13,41], which has an average sea level of 3,900 meters (ASL). The Ürümqi River is a typical intermountain river that is supplemented by glacial meltwater and precipitation [10,25]. Streamflow in this basin is supplied by snowmelt and perennial glacier

melting in spring, apart from rainfall and snowmelt in summer [13,22]. The flood peak season is July and August, mainly from rainfall. Rising air temperature and intensive evapotranspiration has affected the runoff dramatically in the upstream of Ürümqi River [42].

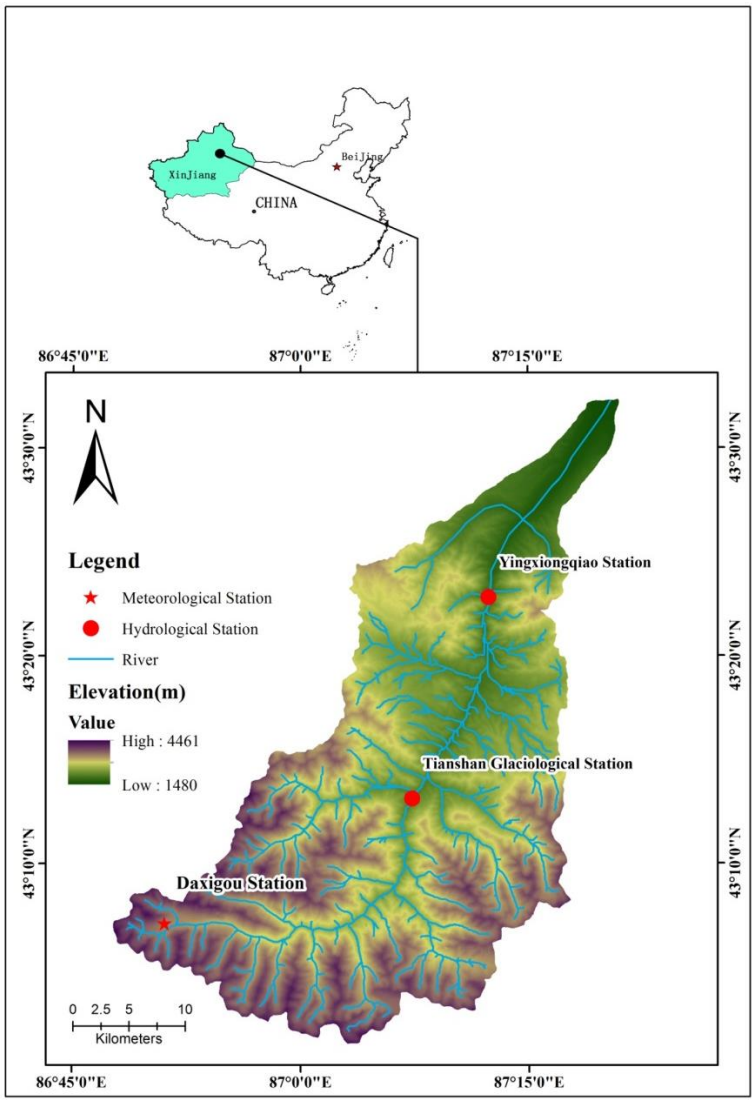


**Figure 1.** The position of hydro-meteorological observation sites and digital elevation map (DEM) of the upstream of the Ürümqi River, Tianshan Mountains, China.

The area is endowed with a complex topography of grasslands, marshes and deserts located next to the surrounding alpine mountains [43]. Data on this basin is limited. In 1958, the Yingxiongqiao Hydrological Gauging Station (YHGS) (figure 1) was set up in the upstream of the Ürümqi River. It is the sole hydrological gauging station with a prolonged series of available data located in the mountain pass. The river above YHGS is about 62.6 km long, covering 924 $km^2$ drainage area at an average altitude of 3483 m ASL (figure 1). The study area (ie above YHGS) falls into three climate zones: 1) Mountain snow area (i.e, modern glacier area) with an average snow line height of 4050 m ASL, annual average temperature of -6 ℃ and 75% of annual precipitation is in the form of snow, 2) The sub-alpine tundra with an annual average temperature of -1.86 ℃ and snowfall makes up 50% of the annual precipitation, 3) High-cold and low-temperature areas with an annual average temperature of

2 ℃ and snowfall makes up 25% of annual precipitation [10].

In the upper reaches of the Ürümqi River, the precipitation concentrates in June to August. Annual Mean Precipitation at Daxigou Meteorological Station (DMS) is 454 mm (from 1958 to 2006) (figure 1), which has been in operation since 1958. The observed annual maximum precipitation is 632 mm (in 1996) in the upstream area. The average annual air temperature changes from -5.2 ℃ to 0 ℃ in the upstream region. The observed upstream average annual runoff is 7.71 $m^3$/sin YHGS. It should be stated that sparse population and hence the human impact (*i.e.*, water resources development) on the upstream of the Ürümqi River was trivial in the overland hydrological process before 2006. To investigate the effect of climate change on the streamflow, the upstream was selected as a target study area.

*2.2. Data*

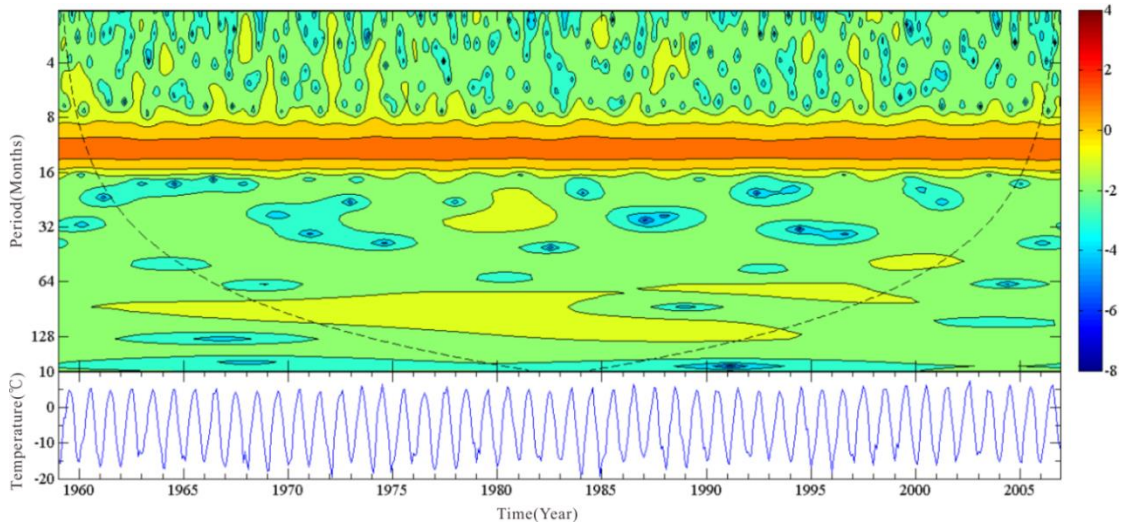


**Figure 2.** Time series (bottom) and continuous wavelet power spectrum (top) of the monthly average air temperature from 1959-2006.

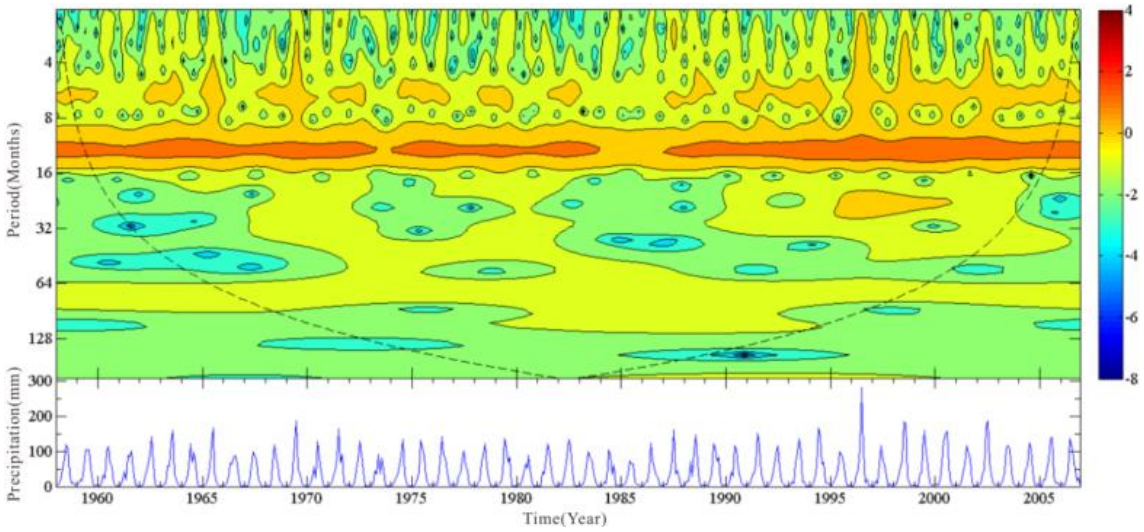


**Figure 3.** Time series (bottom) and continuous wavelet power spectrum (top) of the monthly precipitation from 1959-2006.

Several hydrologic and meteorological datasets for time period of 1958-2006 are used in the study. Monthly average runoff was obtained from YHGS spans for the period from January 1958 to December 2006. Monthly average temperature and precipitation are obtained from DMS for the periods from January 1959 to December 2006 and January 1958 to December 2006 respectively. It should be particularly noted that the Daxigou Reservoir, located 5 km above YHGS, was established in 2007. Its establishment disturbed the natural hydrological conditions of the upstream Ürümqi River, thus YHGS data after 2006 have been omitted from this study. Time series data are shown in figures 2-4.

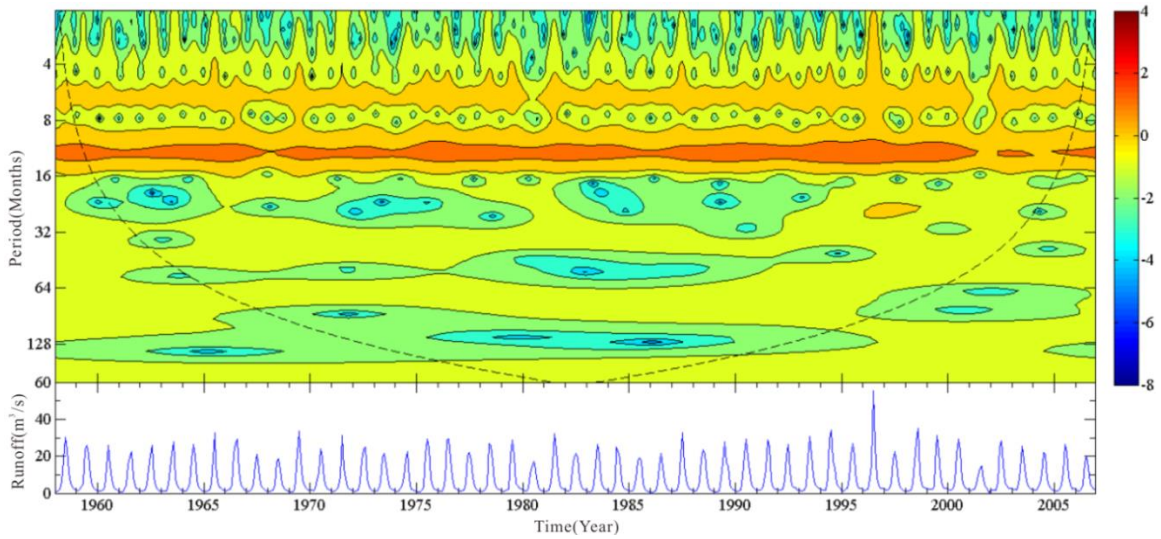


**Figure 4.** Time series (bottom) and continuous wavelet power spectrum (top) of the monthly average runoff from 1959-2006.

## 3. Methods

Wavelet analysis is an effective tool to study the multi-time scale characteristics of hydrological factors [27,30,44]. It can exhibit the periodicities of signals at different time scales. The complex Morlet wavelet (with ω0=6) in the continuous wavelet transform provides a fine balance between time and frequency localization and its Fourier period is almost equal to the scale (λ= 1.03a). Cross wavelet transform and wavelet coherence based on wavelet transform are used to reveal relationships between two signals in time frequency space.

In this study, the Matlab package of cross wavelet and wavelet coherence provided by [28] is used for the calculation and it is available from the URL http://www.pol.ac.uk/home/research/waveletcoherence/.

### *3.1. Morlet continuous wavelet transform*

The continuous wavelet transform is meant to achieve a complete time-scale representation of localized and transient phenomena at different time scales. Coefficients of the wavelet transform of a continuous-time signal $x(t)$ are defined by the linear integral operator

$$C_x(a,\tau)=\int_{-\infty}^{+\infty} x(t)\psi_{a,\tau}^{*}(t)\,\mathrm{d}t \quad \text{with} \quad \psi_{a,\tau}(t)=\frac{1}{\sqrt{a}}\psi\left(\frac{t-\tau}{a}\right) \tag{1}$$

where * represents the complex conjugate. The wavelet function $\psi(t)$ can be either real or complex. The parameter $a$ can be regarded as a dilation ($a>1$) or contraction ($a<1$) factor of the wavelet function $\psi(t)$, in agreement with different scales of observation. The parameter $\tau$ can be

expressed as a temporal or function translation $\psi(t)$, which makes the study of the signal $x(t)$ possible locally around the time $\tau$. In this study, we have selected the complex Morlet wavelet $\psi(t)$ which is defined as follows:

$$\psi(t) = \pi^{-1/4} e^{iw_0 t} e^{-t^2/2} \tag{2}$$

where $w_0$ denotes frequency. The wavelet power spectrum $W_X(a,\tau)$ of a continuous-time signal $x(t)$ is defined as the modulus of its wavelet coefficients:

$$W_X(a,\tau) = C_X(a,\tau) C_X^*(a,\tau) = \left|C_X(a,\tau)\right|^2 \tag{3}$$

The wavelet transformation at a point in time always contains information of neighboring data points. If the center of the wavelet is close to the start or the end of the signal, edge effects will occur. The cone of influence (COI) is the region of the wavelet spectrum where edge effects become important and is defined here as the e-folding time for the auto-correlation of wavelet power at each scale. For the complex Morlet wavelet, the e-folding time is $\sqrt{2}a$. This e-folding time is chosen so that the wavelet power for a discontinuity at the edge decreases by a factor of e-2 and ensures that the edge effect is negligible beyond the point [45]. Therefore, the Morlet wavelet is often selected by researchers for analysis on geophysical time series [27,28,30,32,44]. In addition, the wavelet transform variance is completed to find the significant periods. The peak variance corresponds to significant periods of the signal.

*3.2. Cross wavelet transform and wavelet coherence*

Cross wavelet transform (XWT) and wavelet coherence (WTC) are adopted to illustrate the relationships between runoff and meteorological factors [46]. The wavelet cross-spectrum $W_{XY}(a,\tau)$ between the two signals $x(t)$ and $y(t)$ is defined as:

$$W_{XY}(a,\tau) = C_X(a,\tau) C_Y^*(a,\tau) \tag{4}$$

where $C_X(a,\tau)$ and $C_Y^*(a,\tau)$ represent the wavelet coefficient of the continuous-time signal $x(t)$ and the complex conjugate of the wavelet coefficient of $y(t)$ respectively. The wavelet cross-spectrum $W_{XY}(a,\tau)$ is intended to measure the cross-covariance of the signals $x$ and $y$. It is worth noting that the cross wavelet transform can reveal the common power and relative phase in the time-frequency space, while the WTC can find significant coherence even when the normal power is low [18,47].

Generally speaking, the notion of coherence in signal processing consists of a measure of the correlation between two signals or between two representations of these signals. WTC measures the cross-correlation between two signals as a function of frequency [45]. This highlights the temporal variation in the correlation between the two signals and allows detection of high-transient covariance. The wavelet coherence of two signals is defined as the absolute value squared of the smoothed wavelet cross-spectrum, as normalized by the smoothed wavelet power spectra:

$$WC(a,\tau) = \frac{\left|\left\langle a^{-1} W_{XY}(a,\tau)\right\rangle\right|^2}{\left\langle a^{-1}\left|W_X(a,\tau)\right|\right\rangle \left\langle a^{-1} W_Y(a,\tau)\right\rangle} \tag{5}$$

where $\langle\cdot\rangle$ indicates smoothing both in time and scale, as discussed by Torrence and Webster [48]

and Labat *et al* [47]. The wavelet coherence $WC(a,\tau)$ takes a value between 0 and 1, and is an accurate representation of the (normalized) covariance between the two signals [45].

When the wavelet function is the complex Morlet wavelet, the corresponding wavelet cross-spectrum $W_{XY}(a,\tau)$ is complex as well. The angle tan-1 [imaginary part of $W_{XY}(a,\tau)$ / real part of $W_{XY}(a,\tau)$] is defined as the wavelet coherence phase. A consistent phase relationship in regions with large common power suggests physical causality between two signals.

The statistical significance level of the wavelet coherence is estimated by using Monte Carlo methods and is discussed in detail in [28,45,49].

Two statistical limits are taken into account to restrict our analysis to statistically significant-only fluctuations: 1) Only periodicity is different from red noise [45] within 95% confidence intervals are considered; 2) Because the edge effect produces COI, if $T$ is the total length of the series, periods less than $T/2\sqrt{2}$ will be considered as significant. However, if previous studies have shown oscillations with periods from $T/2\sqrt{2}$ to $T/2$ (Nyquist frequency), these oscillations will be included.

## 4. Results and discussion

### *4.1. Multiple time scale analysis by wavelet spectra*

Changes of runoff in upstream of the Ürümqi River are mainly caused by local climate changes. Air temperature and precipitation datasets are used as climate factors. Firstly, Morlet continuous wavelet transform was performed on climate factors and the runoff to find their significant periodicities.

4.1.1. Wavelet analysis on monthly air temperature. Monthly average air temperature variations from 1959 to 2006 are depicted in figure 2 (bottom). It fluctuates steadily in the range from -19.7 ℃ to 7.4 ℃. Annual average air temperature is -5.1 ℃ and shows a significant upward trend in the past 50 years with an approximate growth rate of 0.2 ℃ per decade. In 1972, 1984, 1985 and 1996, air temperatures were notedly below the average, while air temperatures in 1986 and 2002 were notedly above average.

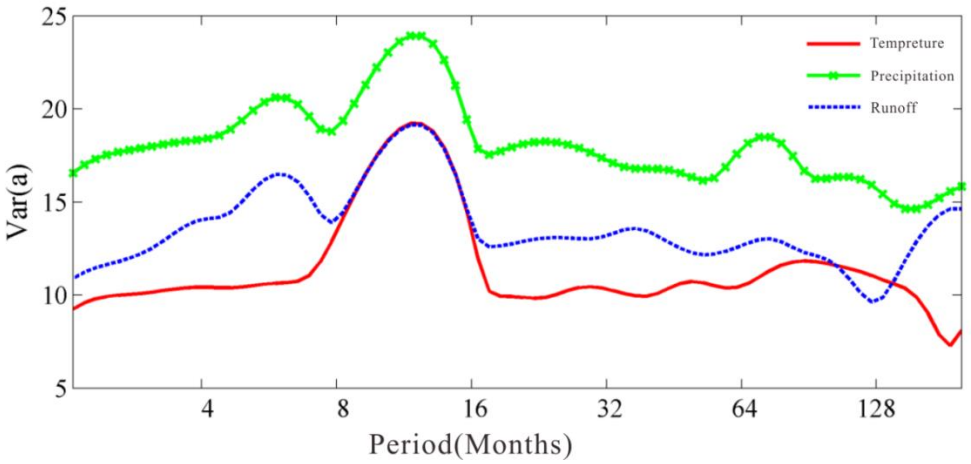


**Figure 5.** Plot of wavelet variance for the monthly average air temperature, monthly precipitation and monthly average runoff.

Figure 2 (top) shows the wavelet power spectrum of monthly average air temperatures. The dashed black line designates the cone of influence. At the 95% significance level, several long periods were detected for the air temperature time series. Air temperature fluctuates significantly at the 12-month cycle over the period of 1959-2006. This cycle can be observed in the wavelet spectrum almost

throughout the entire analytical cycle, and the cycle has always been significant. In addition, four shorter cycles were detected (96, 66, 24 and 48 months). In view of the wavelet power spectra, these low-level cycles are significant only for a short period of time, such as the 96-month scale between the years 1969–1992, 66-month scale between the years 1987–1997, 48-month scale between the years 1998–2002, and 24-month scale between the years 1977–1992. The time series show that these shorter cycles have significant time characteristics. These cycles are also visible in the wavelet variance (figure 5), although they change from time to time. This time period conforms to the year and the daily minimum temperature is usually lower than the long-term average. This means that long cycles have existed for many years, especially during cold winters.

*4.1.2. Wavelet analysis on monthly average precipitation.* Precipitation is one of the main factors affecting the runoff in upstream of the Ürümqi River. Figure 3 (bottom) presents the monthly precipitation time series. It fluctuates between 0-284 mm and is unevenly distributed with 60 percent of the annual precipitation in summer. Inter-annual fluctuations of precipitation are visible, with the minimum annual precipitation at less than 300 mm in 1985 and the maximum at 632 mm in 1996. On the whole, precipitation has a significant increasing trend since the mid-1980s.

In general, the wavelet spectra show a varied behavior of the monthly precipitation time series used to calculate the catchment precipitation series, which depends on the geographic position of climatic stations. However, the wavelet power spectrum is still very effective for the analysis of precipitation time series for specific climatic stations [32]. Figure 3 (top) depicts the wavelet power spectrum of monthly precipitation. Monthly precipitation fluctuates significantly at the narrow 12-month scale band over the observed time period, indicating that there is a significant characteristic of inter-annual variability of monthly precipitation. Precipitation also fluctuated at three different low-level periods, namely 6-month, 30-month and 72-month. The 6-month scale between the years 1960-2005 was mainly for precipitation with the largest impact. The 30-month scale was found over the periods of 1967-1972, 1978-1982 and 1989-2003 intermittently. Precipitation also fluctuated at a relatively long periodicity of 72-month over the period of 1966-1999.

*4.1.3. Wavelet analysis on monthly average runoff.* Figure 4 illustrates the monthly average runoff and its wavelet power spectrum. Runoff occurs mainly in summer because the runoff from June to August accounts for over 70 percent of the annual runoff, where floods seldom occur in spring. Therefore, the monthly average runoff has an uneven distribution. Average monthly runoff in July from 1959 to 2006 was 26.3 $m^3/s$, while that of February was 1.1 $m^3/s$. Moreover, the inter-annual change of runoff has a large fluctuation, e.g., monthly average runoff in July varies from 13.5 to 55.2 $m^3/s$, as shown in figure 4 (bottom). In general, between the 1950s and late 20th century, runoff showed a noted upward trend. However, runoff appears to decrease since the beginning of this century.

The monthly mean runoff shows that about 12 months of periodicity can be observed in the wavelet power spectrum almost during the entire analysis process, as shown in figure 4 (top). Meanwhile, runoff also fluctuates at 6-, 24-, 36-, 72- and 144-month scales cycles. Runoff fluctuation at the 6-month scale is shown with different characteristics for almost the entire duration of the analyzed period, because the runoff is influenced by seasonal variations of climatic factors at this scale. Different characteristics in different time domains have been found in the 24-month scale between the years 1992-2004. It was consistent with the transition to a warmer and more humid climate in the region during the same period. The 36-month and 72-month scales are detected for almost the entire analyzed duration as well. However, in almost all cases, the wavelet power spectral coefficients are approaching 0. This indicates that these two cycles are not significant. The 144-month variability is found in very limited time zones because of the short analysis period.

*4.1.4. Wavelet variance.* When comparing wavelet variance in monthly temperature, precipitation and runoff in time series, we found that the most significant period is the 12-month scale (figure 5). The 6-month and 72-month cycles of monthly average runoff approximately duplicate the monthly

precipitation, rather than the monthly average air temperature, which implies that the runoff in upstream of the Ürümqi River is mainly affected by precipitation at the 6-month and 72-month scales. For the other scale cycles, the significance detected by wavelet variance is consistent with that illustrated by wavelet transform.

4.2. Cross wavelet analysis between climate factors and runoff

In order to analyze the correlation between air temperature and runoff, precipitation and runoff in time-frequency domains, cross wavelet transform and wavelet coherence are calculated between them [50]. The significant tests against red noise are also calculated in cross wavelet transform and wavelet coherence.

4.2.1. Cross wav*elet between air temperature and runoff*. When comparing the cross wavelet transform with squared wavelet coherence between monthly air temperature and monthly average runoff time series, it can be observed that the air temperature and runoff correlate closely at approximately 12-month scale cycle between the years 1960-2005 (figure 6). Moreover, runoff also responds to the variability of air temperature at scales of 6-, 24-, 34-, 36-, 48- and 72-month. The 6-month cycle occurred over 1960-2005. The 24-month scale was found during 1994-2000. The 34-month scale was observed during 1976-1984. The 36-month scale was detected during 1964-1971. The 48-month was distributed over the period 1996-2002 and the 72-month was found over 1972-1996 (figure 6(a)). This is consistent with the findings of other authors, who analyzed the Tianshan runoff and found the 1-, 2-, 4-and 8- year cycles of the Aksu River [21] as well as the 2-, 4- and 8- year cycles on the Yarkand River [38]. Compared to the cross-wavelet transform, the wavelet coherence (figure 6(b)) has a stronger common power in the time-frequency space. The high power is always available in the time series of 12-month period during most of the observation time span. In this period, air temperature leads runoff by around 0 °. However, in the low-frequency area, we can observe a change in the behavior for most of the observation period. In the low-frequency area, where the four cycles are observed, they are all high in power as well. The four cycles are the 24-month between the years 1977-1984 and the years 1993-2000, 36-month between the years 1981-1985, 48-month between the years 1995-2002, and 72-month between the years 1972-1996 respectively. It shows that the air temperature lead time prolongs with increasing runoff periodicity.

From the phase difference in cross wavelet transform and wavelet coherence, the contributions of air temperature to the runoff can be inferred (figure 6). In the high-frequency area, phase difference at the 12-month is almost 0 °, *i.e.*, increasing air temperature tends to enhance glacier-melting within the catchment which replenishes the river efficiently. Yet, the phase difference at 6-month is very unstable, *i.e.*, increasing air temperature may increase or decrease the runoff at this scale [51]. The Ürümqi River is located in alpine inland areas where air temperature is very low and most precipitation is solid, so the time in which precipitation makes an efficient supply for rivers is different in different seasons [52]. On one hand, the river can be replenished by melting glaciers accelerated by rising air temperature. On the other hand, rising air temperature enhances the evapotranspiration, resulting in fewer melting glaciers which can replenish the river [53]. In the low-frequency region, phase difference varies from 120 ° to 150 °, which means a lead time of 4 to 5 years or so. It can be observed that the phase difference is also growing with increasing cycle. It illustrates that continuous rising air temperature inevitably results in exacerbated glacier melting and weakens its ability to replenish the river. As time goes by, the impact will become more significant.

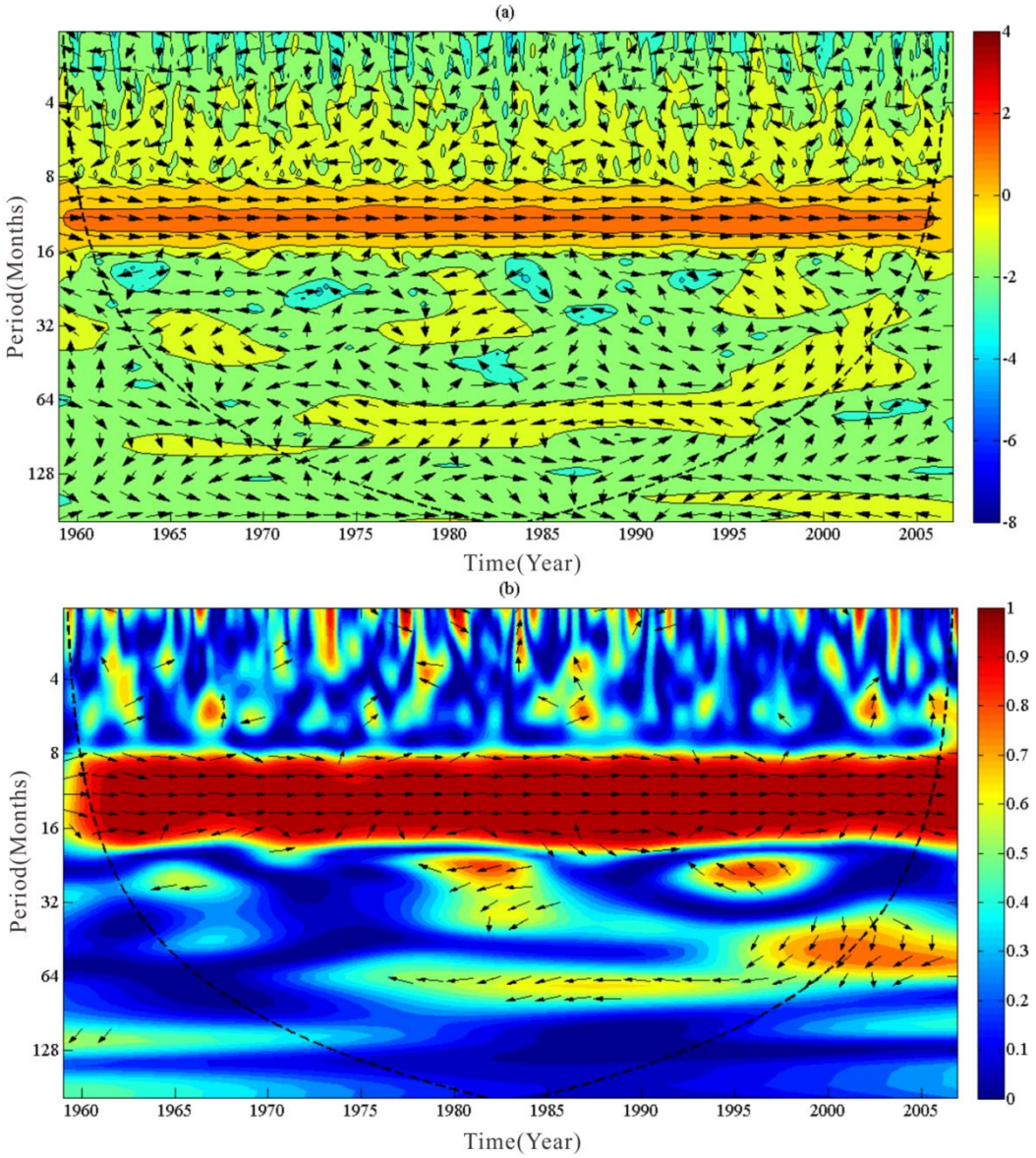


**Figure 6.** Cross wavelet transform (a) and squared wavelet coherence (b) between the monthly average air temperature and monthly average runoff.

*4.2.2. Cross wavelet between precipitation and runoff.* Cross wavelet between monthly precipitation and runoff is depicted in figure 7. It can be observed that for most observation time windows, the significant area of the cross-wavelet spectrum of precipitation and runoff is approximately in the 12-month cycle region. There is a discontinuous significant area of the cross-wavelet spectrum at the 6-month scale for precipitation and runoff. The change of cross-wavelet spectrum at the 6-month scale is relatively stable in the time series before the 1990s. However, we can observe some oscillation in the behavior for cross-wavelet spectrum until the end of the observation period. In the low-frequency area, the significant area of the cross-wavelet spectrum cannot be seen. This means that runoff is affected by the precipitation over several months, yet its influence is very limited for more than one year. This is in line with the watershed characteristics of large gradient in the upper Ürümqi River.

Figure 7(b) shows wavelet coherence of monthly precipitation and runoff. In half of the spectral region, the wavelet coherence is close to 1. The significant coherence area observed in the actual precipitation/runoff time series spectrum can be seen from the cycle scale of 4 months to 16 months in

the first half of the month until the 1990s, and between 4-month and 32-month after 1990s. This time period agrees with years, when annual precipitation was generally higher than the long-term average. This means that the increase of precipitation was a greater influence factor for runoff. Moreover, a 72-month scale cycle was observed between the years 1965-1996. It means that precipitation is the primary factor to influence the runoff continuously on a larger time scale.

The phase difference is shown in cross wavelet transform and wavelet coherence between precipitation and runoff (figure 7). Similar to the spectra of the observed precipitation/ runoff time series, the phase arrows show that precipitation leads discharge for shorter periodicities. In the significantly correlated areas, almost all the phase difference equals to 0 ° or approximately 0 °. Once again, this shows significant coherence of precipitation–runoff or most of the periods at almost the entire time as expected. This is consistent with the high degree of agreement between the decadal variability of precipitation and flow in the upper reaches of the Ürümqi River as found in [10]. Moreover, the Ürümqi River upstream has geomorphologic features such as high altitudes and steep slopes. The evaporation is small as a result of the low air temperature. Therefore, most precipitation tends to create an efficient supply for the Ürümqi River.

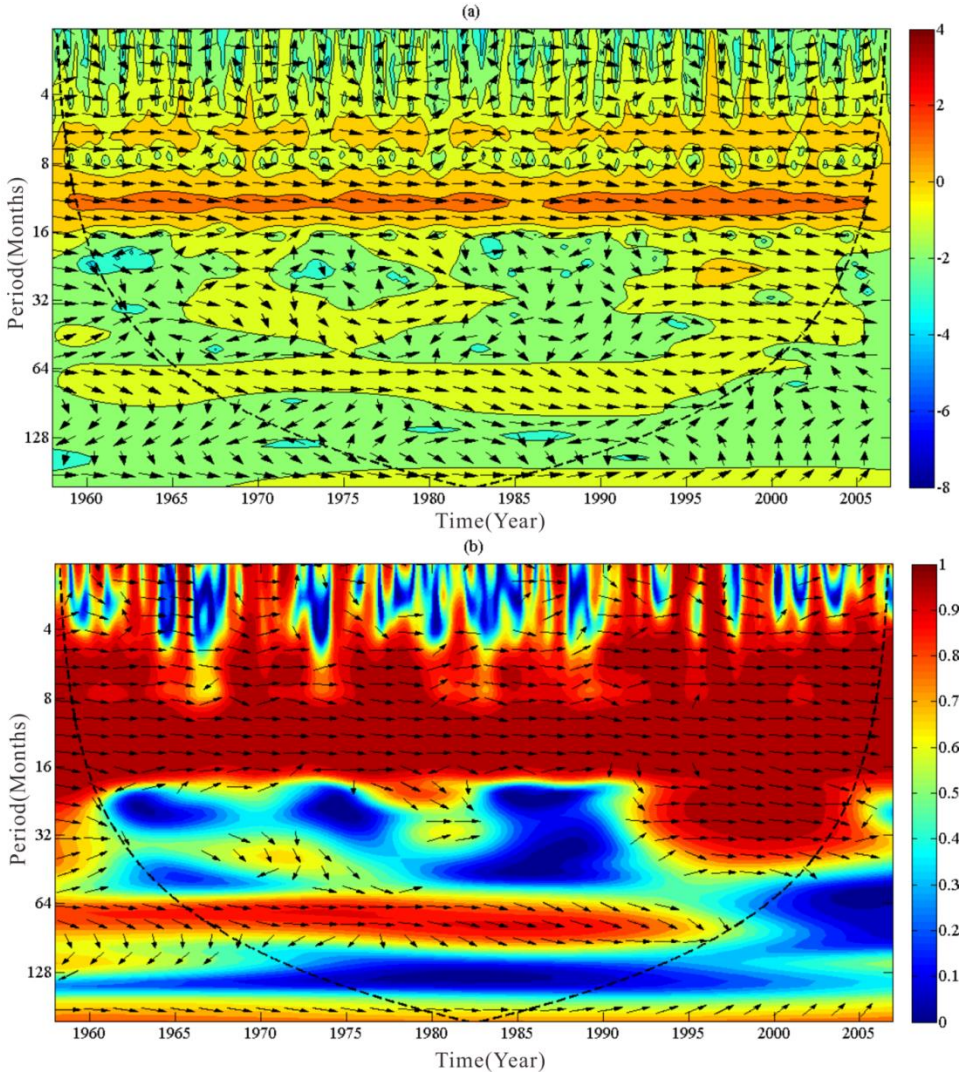


**Figure 7.** Cross wavelet transform (a) and squared wavelet coherence (b) between the monthly precipitation and monthly average runoff.

The main differences between temperature discharges and precipitation discharges can be observed in the cross wavelet transform and wavelet coherence. The precipitation time series show a high degree of consistency in most frequencies and times. On the other hand, the coherence between air temperature and runoff is less significant at most frequencies, except for the high-frequency range. In the temporal periods when the wavelet coherence and the cross-wavelet spectra are closely related to the red noise background, the precipitation and runoff are in positive phase in all cycles, yet the temperature and runoff are in positive phase only at the 12-month scale cycle, while increasing period temperature leads discharge by about 180 °. In other regions the phases are shifted at random.

## 5. Summary and conclusion

The main objective of this article was to conduct an initial analysis on the prolonged behavior of monthly average runoff, air temperature and precipitation time series in the Ürümqi River upstream, as well as to emphasize the long-term cycle and the dependencies of precipitation, temperature and runoff on each other. This large watershed is of the highest importance as water management in this part of China is subject to recent transformations in terms of hydroclimatology and anthropogenic impact.

The wavelet spectra of each observation time series are analyzed. High correlation between the various time series is a major reason for the high level of resemblance between the spectra of each variable. Statistical tests of the wavelet spectra confirmed a 12-month scale cycle in all of the three observed timeseries on a 95% significance level. The 12-month cycle is most obvious in the oscillation of air temperature and is more obvious in runoff than in precipitation. In addition, precipitation and runoff have a common significant cycle of 6-month. Furthermore, other cycles of air temperature, precipitation and runoff revealed by continuous wavelet transform are verified by the wavelet variance.

Relations between air temperature, precipitation and runoff time series are studied using the cross-wavelet spectra and wavelet coherence. Both air temperature and precipitation correlates with runoff mainly at the 6-month and 12-month scale bands. The impact of seasonal climate variations on runoff is revealed. Additionally, air temperature and precipitation affect runoff differently, as implied by phase relationship. Runoff is positively correlated with air temperature at the 12-month scale band. At the 6-month scale, the correlation between runoff and air temperature is unstable because phase angle at this scale shifts from the positive to the negative or vice versa with time. The result is due to the double effects of rising air temperature. On one hand, rising air temperature tends to accelerate glacier melting and hence enhances the replenishment to the river. On the other hand, rising air temperature causes an excess of evapotranspiration and thus results in less supply for the river. Moreover, runoff is negatively or almost negatively related to air temperature at 24-, 34-, 48- and 72-month scale bands. However, runoff is positively correlated with precipitation at all detected scales. In addition, one particularly interesting finding is the lead time between precipitation and runoff found in cross-wavelet spectra. 12-month and 72-month scale cycles are significant and this means that precipitation leads runoff by about 6 months and 72 months. Soil moisture storage and near-surface groundwater have a typical residence time at this order of magnitude. This shows that when long-term decadal fluctuations occur in precipitation and runoff, deeper groundwater reserves are available, while this does not happen for short-term fluctuations. This can be clearly shown in figure 7, where a constant time delay has been applied to generate the discharge in all cycles, so that the lead time does not increase with the cycle. Furthermore, from the 1990s, fluctuations of cycle scales tend to intensify at 6-month. This may also be relevant to the effects of water storage into shallow aquifers due to changes in water balance. The precipitation–runoff wavelet coherence spectrum show significant coherence for most of the periods at almost the entire time series as would be expected, where the significant coherence of the air temperature-runoff is only between the months 8-16. Although long periods could not be detected in the temperature time series, all of these showed a long-term persistence. Hence, the long-range dependence may be caused by some other non-cyclical mechanism or process.

**Acknowledgments**
This work is partially supported by the National Natural Science Foundation of China (41471001 & 41301183), the Scientific Research Foundation for Qingjiang Scholars, Jiangxi University of Science and Technology (JXUSTQJBJ2017002), the Major Basic Research Development Program of Ganzhou (2017) for Youcun Liu, and the Guangdong Provincial Natural Science Foundation (2015A030313852). Furthermore, we would like to thank Prof Shijie Zhong in Colorado University of USA, who had contributed his invaluable insights.

**References**
[1] Burns D A, Klaus J and McHale M R 2007 Recent climate trends and implications for water resources in the Catskill Mountain region, New York, USA *J. Hydrol.* **336** 155-70
[2] Huziy N O, Sushama L, Khaliq M N, Laprise R, Lehner B and Roy R 2013 Analysis of streamflow characteristics over Northeastern Canadianin a changing climate *Climate Dynamics* **40** 1879-901
[3] Bawden A J, Linton H C, Burn D H and Prowse T D 2014 A spatiotemporal analysis of hydrological trends and variability in the Athabasca River region, Canada *J. Hydrol.* **509** 333-42
[4] Kalra A and Ahmad S 2012 Estimating annual precipitation for the Colorado River Basin using oceanic-atmospheric oscillations *Water Resour. Res.* **48** W06527
[5] Wilby R L and Harris I 2006 A framework for assessing uncertainties in climate change impacts: Low-flow scenarios for the River Thames, UK *Water Resour. Res*. **42** W02419
[6] Ding Y, Ye B, Han T, Shen Y and Liu S 2007 Regional difference of annual precipitation and discharge variation over west China during the last 50 years *Earth Sci.* **50** 936-45
[7] Lavado Casimiro W S, Ronchail J, Labat D, Espinoza J C and Guyot J L 2012 Basin-scale analysis of rainfall and runoff in Peru (1969–2004): Pacific, Titicaca and Amazonas drainages *Hydrol. Sci. J.* **57** 625-42
[8] Immerzeel W W, Petersen L, Ragettli S and Pellicciotti F 2014 The importance of observed gradients of air temperature and precipitation for modeling runoff from a glacierized watershed in the Nepalese Himalayas *Water Resour. Res.* **50** 2212-26
[9] Liu Y, Wu J, Liu Y, Hu B X, Hao Y, Huo X, Fan Y, Yeh T J and Wang Z L 2015a Analyzing effects of climate change on streamflow in a glacier mountain catchment using an ARMA model *Quat Int* **358** 137-45
[10] Sabzevari A A, Zarenistanak M, Tabari H and Moghimi S 2015 Evaluation of precipitation and river discharge variations over southwestern Iran during recent decades *J. Earth System Sci.* **124** 335-52
[11] Stocker T F, Qin D, Plattner G K, Tignor M M B, Allen S K, Boschung J, Nauels A, Xia Y, Bex V and Midgley P M 2013 *Climate change 2013: The physical science basis. Intergovernmental Panel on Climate Change, Working Group I Contribution to the IPCC Fifth Assessment Report (AR5)* (New York: Cambridge University Press)
[12] Liu Y, Huo X, Liu Y, Hao Y, Fan Y, Zhong Y and Yeh T J 2015b Analyzing monthly average streamflow extremes in the upper Ürümqi River based on a GPD model *Environ. Earth Sci.* **74** 4885-95
[13] Hamlet A F, Mote P W, Clark M P and Lettenmaier D P 2005 Effects of temperature and precipitation variability on snowpack trends in the Western United States *Am. Meteorol. Soc*. **18** 4545-61
[14] Huss M, Farinotti D, Bauder A and Funk M 2008 Modeling runoff from highly glacierized alpine drainage basins in a changing climate *Hydrol. Process.* **22** 3888-902
[15] Stewart L T 2009 Changes in snowpack and snowmelt runoff for key mountain regions *Hydrol. Process.* **23** 78-94
[16] Kundzewicz Z W, Merz B, Vorogushyn S, Hartmann H, Duethmann D, Wortmann M, Huang S H, Su B, Jiang T and Krysanova V 2015 Analysis of changes in climate and river discharge

with focus on seasonal runoff predictability in the Aksu River Basin *Environ. Earth Sci.* **73** 501-16
[17] Singh P and Jain S K 2002 Snow and glacier melt in the Satluj River at Bhakra Dam in the western Himalayan region *Hydrol. Sci. J.* **47** 93-106
[18] Wang Y, Wang X, Li C, Wu F, Yang Z and Yang Z 2015 Spatiotemporal analysis of temperature trends under climate change in the source region of the Yellow River, China *Theor. Appl. Climatol.* **119** 123-33
[19] Chen Y, Takeuchi K, Xu C, Chen Y and Xu Z 2006 Regional climate change and its effects on river runoff in the Tarim Basin, China *Hydrol. Process.* **20** 2207-16
[20] Xu J, Chen Y, Lu F, Li W, Zhang L and Hong Y 2011 The nonlinear trend of runoff and its response to climate change in the Aksu River, western China *Int. J. Climatol.* **31** 687-95
[21] Cui Y, Ye B, Wang J and Liu Y 2013 Influence of degree-day factor variation on the mass balance of glacier No. 1 at the headwaters of Ürümqi River, China *J. Earth Sci.* **24** 1008-22
[22] Shi Y, Qu Y, Ma S, Chen L, Yuan Z, Tang Y and Huang W 1992 *Bearing Capacity and Rational Utilization of Water Resources of Ürumqi River Basin* (Beijing, China: Science Press) (In Chinese)
[23] Liu H, Bao A, Chen X, Wang L and Pan X 2011 Response analysis of rainfall–runoff processes using wavelet transform: a case study of the alpine meadow belt *Hydrol. Process.* **25** 2179-87
[24] Li Z, Wang W, Zhang M, Wang F and Li H 2010 Observed changes in streamflow at the headwaters of the Ürümqi River, Eastern Tianshan, Central Asia *Hydrol. Process.* **24** 217-24
[25] Barnett T P, Adam J C and Lettenmaier D P 2005 Potential impacts of a warming climate on water availability in snow-dominated regions. *Nat.* **438** 303-9
[26] Lafrenière M and Sharp M 2003 Wavelet analysis of inter-annual variability in the runoff regimes of glacial and nival stream catchments, BowLake, Alberta *Hydrol. Process.* **17** 1093-118
[27] Grinsted A, Moore J C and Jevrejeva S 2004 Application of the cross wavelet transform and wavelet coherence to geophysical time series *Nonlinear Process. Geophys.* **11** 561-6
[28] Labat D 2008 Wavelet analysis of the annual discharge records of the world'slargest rivers *Adv. Water Resour.* **31** 109-17
[29] Labat D 2010 Cross-wavelet analyses of annual continental freshwater discharge and selected climate indices *J. Hydrol.* **385** 269-78
[30] Schaefli B, Maraun D and Holschneider M 2007 What drives high flow events in the Swiss Alps? Recent developments in wavelet spectral analysis and their application to hydrology *Adv. Water Resour.* **30** 2511-25
[31] Szolgayova E, Parajka J, Blöschl G and Bucher C 2014 Long term variability of the Danube River flow and its relation to precipitation and air temperature *J. Hydrol.* **519** 871-80
[32] Jiang Y, Zhou C and Cheng W 2007 Streamflow trends and hydrological responseto climatic change in Tarim headwater basin *J. Geogr. Sci.* **17** 51-61
[33] Nalley D, Adamowski J and Khalil B 2012 Using discrete wavelet transforms to analyze trends in streamflow and precipitation in Quebec and Ontario (1954–2008) *J. Hydrol.* **475** 204-28
[34] Partal T 2012 Wavelet analysis and multi-scale characteristics of the runoff and precipitation series of the Aegean region (Turkey) *Int. J. Climatol.* **32** 108-20
[35] Labat D, Espinoza J C, Ronchail J, Cochonneau G, de Oliveira E, Doudou J C and Guyot J L 2012 Fluctuations in the monthly discharge of Guyana Shield rivers, related to Pacific and Atlantic climate variability *Hydrol. Sci. J.* **57** 1081-91
[36] Qian K, Wang X S, Lv J and Wan L 2014 The wavelet correlative analysis of climatic impacts on runoff in the source region of Yangtze River, in China *Int. J. Climatol.* **34** 2019-32
[37] Xu J, Chen Y, Li W, Nie Q, Song C and Wei C 2014 Integrating wavelet analysis and BPANN to simulate the annual runoff with regional climate change: a case study of Yarkand River, Northwest China *Water Resour. Manage.* **28** 2523-37

[38] Liu Y, Metivier F, Gaillardet J, Ye B, Meunier P, Narteau C, Lajeunesse É, Han T and Malverti L 2011 Erosion rates deduced from seasonal mass balance along the upper Ürümqi River in Tianshan *Solid Earth* **2** 283-301
[39] Sorg A, Bolch T, Stoffel M, Solomina O and Beniston M 2012 Climate change impacts on glaciers and runoff in Tien Shan (Central Asia) *Nat. Clim. Chang.* **12** 725-31
[40] Metivier F, Meunier P, Moreira M, Crave A, Chaduteau C, Ye B and Liu G 2004 Transport dynamics and morphology of a high mountain stream during the peak flow season: The Ürümqi River (Chinese Tianshan) *River Flow* **11** 761-77
[41] Duan K, Yao T, Wang N and Liu H 2012 Numerical simulation of Ürümqi Glacier No. 1 in the eastern Tianshan, central Asia from 2005 to 2070 *Chin. Sci. Bull.* **57** 4505-9
[42] Liu Z, Liu Y, Hao Y, Han T, Cui Y, Wang J and Wang Z 2014 Multi-time scale cross-wavelet transformation between runoff and climate factors in the Upstream of Heihe River *J. Arid Land* **37** 1137-46 (in Chinese).
[43] Labat D 2005 Recent advances in wavelet analyses: Part 1. A review of concepts *J. Hydrol.* **314** 275-88
[44] Torrence C and Compo G P 1998 A practical guide to wavelet analysis *Bull. Am. Meteorol. Soc.* **79** 61-78
[45] Liu P C 1994 Wavelet spectrum analysis and ocean wind waves *Wavelets in Geophysics* pp 151-66 (New York: Academic Press)
[46] Labat D, Ababou R and Mangin A 2000a Rainfall–runoff relations for karstic springs. Part I: convolution and spectral analyses *J. Hydrol.* **238** 123-48
[47] Torrence C and Webster P J 1999 Interdecadal changes in the ENSO-Monsoon system *J. Clim.* **12** 2679-90
[48] Labat D, Ababou R and Mangin A 2000b Rainfall–runoff relations for karstic springs. Part II: continuous wavelet and discrete orthogonal multiresolution analyses *J. Hydrol.* **238** 149-78
[49] Xu J H, Chen Y N, Li W H, Ji M H, Dong S and Hong Y L 2009 Wavelet analysis and nonparametric test for climate change in Tarim River Basin of Xinjiang during 1959-2006 *Chin. Geogr. Sci.* **19** 306
[50] Kong Y and Pang Z 2017 What is the primary factor controlling trend of Glacier No. 1 runoff in the Tianshan Mountains: temperature or precipitation change? *Hydrol. Res.* **48** 231-9
[51] Zhang S Q and Pu Z C 2011 Analysis of spatial and temporal change of precipitation in Ürümqi River Basin based on DEM *Chin. J. Agrometeorol.* **32** 437-43
[52] Zhang Y, Luo Y and Sun L 2016 Quantifying future changes in glacier melt and river runoff in the headwaters of the Ürümqi River, China *Environ. Earth Sci.* **75** 770